Numerical Simulation of Natural Gas-Swirl Burner

FINAL TECHNICAL REPORT

9/30/2001 through 12/31/2004

Dr. Ala Qubbaj, Mechanical Engineering Department

March 2005

DE-FG26-01NT41364

University of Texas pan American
1201 West University Drive
Edinburg, Texas 78539-2999

DISCLAIMER NOTICE

This report was prepared as an account of work sponsored by an agency of the United States Government. Neither the United States Government nor any agency thereof, or any of their employees, makes any warranty, express or implied, or assumes any legal liability or responsibility of the accuracy, completeness, or usefulness of any information, apparatus, product, or process disclosed, or represents that its use would not infringe privately owned rights. Reference herein to any specific commercial product, process, or service by trade name, trademark, manufacturer, or otherwise does not necessarily constitute or imply its endorsement, recommendation, or favoring by the United States Government or ant agency thereof. The views and opinions of authors expressed herein do not necessarily states or reflect those of the United States Government or ant agency thereof.

ABSTRACT

A numerical simulation of a turbulent natural gas jet diffusion flame at a Reynolds number of 9000 in a swirling air stream is presented. The numerical computations were carried out using the commercially available software package CFDRC. The instantaneous chemistry model was used as the reaction model. The thermal, composition, flow (velocity), as well as stream function fields for both the baseline and air-swirling flames were numerically simulated in the near-burner region, where most of the mixing and reactions occur. The results were useful to interpret the effects of swirl in enhancing the mixing rates in the combustion zone as well as in stabilizing the flame**.** The results showed the generation of two recirculating regimes induced by the swirling air stream, which account for such effects. The present investigation will be used as a benchmark study of swirl flow combustion analysis as a step in developing an enhanced swirl-cascade burner technology.

TABLE OF CONTENTS

A. INTRODUCTION

The primary objectives in burner design are to increase combustion efficiency and to minimize the formation of environmentally hazardous emissions such as nitrogen oxides (NO_x) and carbon monoxide (CO). Critical design factors that impact combustion include: the temperature and residence time of the combustion zone, the initial temperature of the combustion air, the amount of excess air and turbulence in the burner, and the manner in which the air and fuel streams are delivered and mixed. Elevated temperatures and excess air contribute to better burning of the fuel but lead to high levels of NO_x. Lower temperatures and fuel-rich mixtures produce incomplete (inefficient) combustion, which lead to elevated levels of CO. The design of a good burner thus involves finding an optimal balance between these conflicting requirements. In this respect, CFD can serve as a powerful tool.

Different technologies to control pollutant emissions from combustion systems (particularly NOx) have been developed. Flue Gas Recirculation (FGR), water injection, after burning, selective catalytic reduction (SCR), and non-catalytic reduction (SNCR), are active post combustion techniques that have been employed [1,2]. On the other hand, passive techniques to manipulate the flow dynamics and rates of mixing of reactants in the combustion zone have been the focus of research in the last decade. The application of non-axisymmetric burner-exit geometries [3-5], staging of fuel-air mixing [6], swirl burners [7,8], as well as venturi-cascading [9,10] are examples of such techniques.

"Venturi-cascading" technique was developed by Qubbaj and Gollahalli [9,10] in the last three years. The basic idea behind this technique is controlling the stoichiometry of the flame through changing the flow dynamics and rates of mixing in the combustion zone with a set of venturis surrounding the flame. Venturi-cascading has shown advantages over other techniques; its reliability, flexibility, safety, and cost makes it more attractive and desirable. However, it has resulted in a moderate pollutant emissions reduction compared to SCR, SNCR and FGR methods.

Swirl combustion has shown superiority over other techniques as well; it meets a further important design objective of producing a stable flame under a variety of operating conditions and fuel types. The basic idea is to impart swirl to the air or fuel stream, or both. This not only helps to stabilize the flame but also enhances mixing in the combustion zone. As a result, nonpremixed (diffusion) swirl burners have been increasingly used in industrial

combustion systems such as gas turbines, boilers, and furnaces, due to their advantages of safety and stability, and consequently have a strong influence on flame emissions.

Previous studies have reported significant improvements in the combustion and emission characteristics of combustion systems utilizing swirl flow configurations [7,8,11-14]. Nevertheless, the interaction between such improvements and the flow field characteristics (including mixing and recirculation) still is to be understood. In many combustion devices both reactants are in gas phase and for technological reasons the coaxial geometry is commonly used to merge the two streams [15]; the swirl motion is used to improve flame stability and enhance mixing processes [13,16].

The general goal of the current research is the improvement and optimization of the mixing processes between the reactants in such a way to minimize the environmental impact of combustion systems. Any improvement in the combustion performance relative to pollutant formation, stability, and overall efficiency requires a careful study of the flow field and mixing processes, particularly in such a highly turbulent reacting flow. The scaling of pollutant emissions in industrial flames is very difficult because of the complex geometry of the burner and the many parameters involved. The experimental evidence is that each burner is a unique device and even small geometry changes can influence the level of emissions. Earlier studies showed that swirl flows require a detailed flow structure and specification of the inlet conditions [17-19]. The fluid dynamic analysis is very useful to provide the preliminary information about the mixing process. Therefore, in this benchmark study, CFD simulations will be used to acquire a close understanding of the flow, thermal, and composition fields in the primary mixing zone produced by swirl in a turbulent non-premixed swirling combustor. As a result, the interaction of the flow field characteristics (including mixing and recirculation) with the combustion and emission characteristics will be delineated. The present investigation will be used as benchmark study of swirl flow combustion analysis as precursor to develop an enhanced swirl-cascaded burner technology.

B. PHYSICAL MODEL

Figure 1(a) shows the actual physical model, which consists mainly of a combustion chamber made from steel, 63.5 cm x 63.5 cm cross-section and 139.7 cm height. The chamber is provided with air-cooled Pyrex windows of dimensions 38.1 cm x 114.3 cm on

all four sidewalls. The top of the chamber is connected to the atmosphere through an exhaust duct (as seen in Fig. 1). The fuel and oxidant are introduced to the combustion chamber through separate streams in a non-premixed or diffusion combustion process. The fuel is introduced through a stainless steel burner, of internal diameter 3.2 mm, inserted in the centerline of the chamber, and the air is introduced through an annular inlet of diameter 0.2 m, surrounding the fuel burner as depicted in Figure 1. Swirl is imparted to the air stream at swirl number (level) 1. The swirl number represents the ratio between the angular and axial air velocities. The simplified physical model used in the computations, assuming axisymmetric flow conditions, is provided in Fig 2. The operating and boundary conditions are given in Table 1.

Table 1: Operating and Boundary Conditions

Fuel	Natural Gas (95%+)
Burner diameter (d)	3.175 mm
Jet-exit Reynolds number	9000
Jet-exit/ Fuel axial velocity u_x	46.65 m/s
Swirl number (rw/U)	1.0
Angular air velocities u_θ	3 m/s
Axial air velocity u_x	0.3 m/s
Near-burner axial location: x/d	4.63
Ambient temperature	295 K
Ambient pressure	100 kPa

C. NUMERICAL COMPUTATIONS

Computational Model

The numerical computations were conducted using the *CFDRC-ACE+*, advanced computational environment software package 2001, in which CFD-GEOM (Interactive Geometric Modeling and Grid Generation software) and CFD-VIEW (3-D Computer Graphics and Animation Software) are incorporated. The computational domain encompassed half of the flame jet assuming axisymmetric flow conditions (as seen in Fig. 2) and extended to 139.7 cm in the axial direction and 31.75 cm in the radial direction. The grid cells were generated with increasing spacing in the radial and axial directions; this

provided an adequate resolution where gradients were large, i.e., near the centerline, and saved CPU time where gradients were small, near the edges.

A cell-centered control volume approach was used, in which the discretized equations or the finite difference equations (FDE) were formulated by evaluating and integrating fluxes across the faces of control volumes in order to satisfy the Favre-averaged continuity, momentum, energy and mixture fractions conservation equations (Eqs. 1, 2, 4 and 9, respectively). The first order upwind scheme was used for evaluating convective fluxes over a control volume. The well-known SIMPLEC algorithm, proposed by Van Dooormal and Raithby [20], was used for velocity pressure-coupling. SIMPLEC stands for "Semi-Implicit Method for Pressure-Linked Equation Consistent", in which an equation for pressure correction is derived from the continuity equation. The standard k-ε model was used to close the set of equations.

Governing Equations

The code CFD-ACE+ employs a conservative finite-volume methodology and accordingly all the governing equations are expressed in a conservative form in which tensor notation is generally employed. The basic governing equations are for the conservation of mass, momentum and energy:

Continuity equation:

$$\frac{\partial \rho}{\partial t} + \frac{\partial}{\partial x_j}(\rho u_j) = 0 \quad \text{.....} \quad (1)$$

where u_j is the j^{th} Cartesian component of velocity and ρ is the fluid density.

Momentum equations: (j=1, 2, 3)

$$\frac{\partial}{\partial t}(\rho u_j) + \frac{\partial}{\partial x_i}(\rho u_i u_j) = -\frac{\partial p}{\partial x_j} + \frac{\partial \tau_{ij}}{\partial x_i} + \rho f_j \quad \text{.....} \quad (2)$$

where p is the static pressure, τ_{ij} is the viscous stress tensor and f_j is the body force. For Newtonian fluids τ_{ij} can be expressed as:

$$\tau_{ij} = \mu\left(\frac{\partial u_i}{\partial x_j} + \frac{\partial u_j}{\partial x_i}\right) - \frac{2\mu}{3}\left[\frac{\partial u_k}{\partial x_k}\right]\delta_{ij} \quad \text{.....} \quad (3)$$

where μ is the fluid dynamic viscosity and δ_{ij} is the Kronecker delta.

Energy Equation:

The equation for the conservation of energy can take several forms. The static enthalpy form of the energy equation can be expressed as:

$$\frac{\partial}{\partial t}(\rho h)+\frac{\partial}{\partial x_j}(\rho u_j h)=-\frac{\partial q_j}{\partial x_j}+\frac{\partial p}{\partial t}+u_j\frac{\partial p}{\partial x_j}+\tau_{ij}\frac{\partial u_i}{\partial x_j}-\frac{\partial}{\partial x_j}(J_{mj}h_m) \quad \text{.......(4)}$$

where J_{mj} is the total (concentration-driven + temperature-driven) diffusive mass flux for species m, h_m represents the enthalpy for species m, and q_j is the j-component of the heat flux. J_{mj}, h_m and h are given as:

$$J_{mj}=-\rho D\frac{\partial Y_m}{\partial X_j} \quad \text{..............................(5)}$$

$$h_m=\int_{T_o}^{T} C_{P_m}(T)dT+h^o_{f_m} \quad \text{..............................(6)}$$

$$h=\sum_{m=1}^{n} Y_m h_m \quad \text{..............................(7)}$$

where D is the diffusion coefficient, C_p is the constant-pressure specific heat, and h_f^o is the enthalpy of formation at standard conditions (P_o=1 atm, T_o=298 K).

The Fourier's law is employed for the heat flux:

$$q''_j=-K\frac{\partial T}{\partial x_j} \quad \text{..............................(8)}$$

where K is the thermal conductivity.

Mixture Fractions:

$$\frac{\partial}{\partial t}(\rho f_k)+\frac{\partial}{\partial x_j}(\rho u_j f_k)=\frac{\partial}{\partial x_j}\left(D\frac{\partial f_k}{\partial x_j}\right) \quad \text{..............................(9)}$$

where D is the diffusion coefficient, f_k is the mixture fraction for the k^{th} mixture.

Chemistry/Reaction Model

The reaction model used by CFD-ACE+ was the instantaneous chemistry model in which the reactants are assumed to react completely upon contact. The reaction rate is infinitely rapid and one reaction step is assumed. Two reactants, which are commonly referred to as

"fuel" and "oxidizer", are involved. A surface "flame sheet" separates the two reactants (this assumption can be made only for nonpremixed flames). The mass fractions for this model are computed by first using Eq. 10 to obtain the composition that would occur without the reaction. The "unreacted" composition, denoted by the superscript "u", is given by

$$(Y_i)^u = \sum_{k=1}^{K} \xi_{ik} f_k \quad \text{.....(10)}$$

where ξ_{ik} is the mass fraction of the i^{th} species in the k^{th} mixture, Y_i is the mass fraction of the i^{th} species and f_k is the mixture fraction of the k^{th} mixture. The change in composition due to the instantaneous reaction is then added to the unreacted mass fractions, as described below.

A stoichiometrically correct reaction step needs to be specified. The mass of species i produced per unit mass of fuel consumed is

$$r_i = -\frac{\nu_i M_i}{\nu_f M_f} \quad \text{.....(11)}$$

where ν is the stoichiometric coefficient of the species in the overall reaction; positive for product species and negative for fuel and oxidizer. The instantaneous reaction mechanism consumes either all the fuel or all the oxidizer, whichever is limiting. The amount of fuel consumed is

$$\Delta Y_f = \min\left(\frac{(Y_f)^u}{-r_f}, \frac{(Y_{ox})^u}{-r_{ox}}\right) \quad \text{….....(12)}$$

The change in each species due to the reaction is proportional to the change in fuel, with the proportionality constant given by Eq. 11. The mass fraction of each species is then given by

$$Y_i = (Y_i)^u + r_i \Delta Y_f \quad \text{.....(13)}$$

The right-hand side of the above equation is only a function of the K mixture fractions. Therefore, K-1 transport equations were solved for the mixture fractions. These equations have no source terms due to chemical reactions.

In this analysis no chemistry model is introduced for the prediction of NO_x formation, and nitrogen is assumed to be chemically inert. NO_x is typically present in very low concentrations in the range of tens to hundreds of parts-per-million (ppm) and therefore has

a negligible impact on the major physico-chemical process in combustion. Moreover, NO_x chemistry is orders of magnitude slower compared to the reaction rate of the fuel. NO_x formation is therefore not directly influenced by turbulent mixing; rather it is influenced by mean concentration levels of the primary constituents in the mixture. For this reason, NO_x related computations are typically done in a post-processing phase. Even without a NO_x model, often very useful qualitative information can be gained by studying various aspects of the numerical solution. For example, a high flame temperature and excess amounts of oxygen in the exhaust gases may be indicative of high NO_x emission levels.

D. RESULTS AND DISCUSSION

Figure 2 shows the radial temperature profiles for both baseline and air-swirling flames in the near burner region, which corresponds to an axial location of x/d=4.63. This near burner region is of primary interest in this study since this is the area where most of the mixing and reactions take place. From the temperature profiles, the following observations can be made: (i) the off-axis peak exists in both cases, however, its radial location moves further inward in the case of swirl; (ii) the peak temperature of the air-swirling flame drops by 8% from its baseline value; (iii) the swirl profile is shifted inward towards the fuel-rich side of the flame; (iv) the air-swirling flame has significantly lower temperatures in the fuel-lean side of the flame, compared to the baseline case. However, it has higher valley temperatures in the fuel-rich side.

The observed shift of the temperature profile towards the fuel-rich side of the flame is a result of the air-swirling effect which produces a recirculation regime as will be seen in Figs. 6 and 7. This recirculation zone sustains the entrainment process of the air stream into the fuel stream, thereby leading to a rapid homogenization of the mixture and the consequent shift of the stoichiometric contour towards the center of the flame. This leaning process has two different effects on the fuel-lean and fuel-rich sides of the flame; the temperature of the latter increases while that of the former decreases. The valley temperature increase in the fuel-rich side of the swirling flame is a result of higher oxygen availability, which pushes the mixture towards stoichiometry. On the other hand, the temperature decrease in the lean side is due to the excess air, which drives the mixture far away from stoichiometry. The net

effect of the swirl on the flame temperature is determined by the resultant of the two aforementioned factors.

Figure 3 depicts the radial concentration profiles of CO_2 at the same conditions pertaining to the earlier temperature profiles. The existence of off-axis peaks, their radial locations, the inward shift of the profiles, the CO_2 increase in the fuel rich side and decrease in the fuel-lean side, all follow the temperature profiles and similar explanations apply. This is reasonable, since CO_2 is a direct combustion product, which depends primarily on temperature and stoichiometry of the flame.

Figure 4 shows the O_2 radial concentration profiles for the baseline and air-swirling flames in the near-burner region. From these profiles the following can be observed: (i) the O_2 concentration starts with a zero value at the central axis and starts to build up in the radial outward direction until it attains its atmospheric value (~21%) near the outside boundary of the flame; (ii) O_2 concentration in the air-swirling flame builds up faster and consequently attain the ambient value earlier than the baseline ones; (iii) O_2 profile in the air-swirling flame is shifted inward, similar to what has been observed earlier for temperature and CO_2 profiles.

The zero O_2 concentration observed in the fuel-rich region is consistent with the absence of CO_2 values observed earlier in the same region. The faster build-up rate in the air-swirling flame compared to the baseline flame is a clear indication of the higher rates of mixing with air provided by the swirling air stream. The average increase of O_2 in the swirling flame compared to the baseline case is the direct cause of the temperature drop observed earlier. The inward shift of the profiles has been noticed for earlier temperature and CO_2 profiles too, and therefore the same aforementioned explanation applies.

Figure 5 shows the radial profiles of the axial velocity component (U) for the baseline and air-swirling flames in the near burner region. These profiles reveal that the air-swirling flame has a lower centerline velocity and a wider profile than the baseline flame. The lower centerline velocity in the air-swirling case suggests a shorter flame by the swirl effect. The effect of swirl is small in the fuel-rich region of the flame; the highest effect is observed in the fuel-lean regions.

In general, for a circular jet, the centerline velocity decreases and the jet becomes wider as the jet grows downstream due to the viscous shear and more air entrainment. Therefore,

the lower centerline velocity and wider profiles observed for the air-swirling flame compared to the baseline flame, are indications of the rapid and faster growth of the gas jet flame in the swirling air stream. However, this interpenetration process is due not to shear but rather to a recirculation bubble (zone) in the vicinity of the fuel jet exit induced by the swirl as seen in Figs. 6 and 7. That recirculation region sustains the entrainment process of the outer air stream into the inner fuel stream. The recirculating regime also presents the capability of an efficient mixing between the streams in the regions near the fuel outlet, therefore leading to a rapid homogenization of the combustible mixture and a shortening of the flame. The higher O_2 concentration and lower axial centerline velocity, observed in Figs. 4 and 5 for the swirl case compared to the baseline case, substantiate the last argument for a shorter flame.

Figure 6 presents the transverse profiles of the radial velocity component (V) at the same conditions. The general trend for the baseline profile is that the radial velocity is zero at the centerline, then it increases to attain a peak value in the fuel-rich region, beyond which it starts decreasing until it reaches a minimum (negative) value close to the stoichiometric contour, then it starts increasing again in the fuel-lean side of the flame to attain an asymptotic value near the flame edge. The positive velocities observed close to centerline imply an outward velocity direction due to jet momentum. On the other hand, the negative velocities noticed farther from the centerline indicate an inward velocity direction. The swirling profile reveals a well pronounced two recirculation zone structure: an internal recirculation zone (IRZ), characterized by negative values of the velocity caused by the adverse pressure gradient induced by the intense swirl, and an external recirculation zone (ERZ) characterized by positive values of velocities. A net increase in the inward radial velocities compared to the outward velocities is observed due the effect of swirl.

Fig. 7 shows the stream function contours which help in interpreting Fig. 6 and visualizing the overall impact of swirl. The swirling air stream fans out on entry into the burner. This produces a low-pressure region immediately downstream of the inlets and causes a massive flow reversal in this region. The streamlines indicate two recirculating zones: the so-called internal recirculation zone (IRZ) produced by the strong swirl, and the external recirculation zone (ERZ), which results from the geometric expansion of the flow.

The IRZ enhances mixing between the fuel and air streams, whereas the ERZ helps to stabilize the flame.

E. CONCLUSIONS

The present study has revealed that introducing swirl to the co-flowing air stream results in the following:

- Flame stabilization due to an external recirculation zone, which results from the geometric expansion of the flow
- An efficient fuel/air mixing in the combustion zone due to an internal recirculation zone induced by the swirling air stream in the vicinity of the fuel jet
- A shorter flame length as indicated by lower centerline axial velocity and higher O_2 in-flame concentrations
- Low NOx emission levels implied by moderate temperatures and less residence time of the flame.

F. REFERENCES

1. Bowman, Craig. T., 1992, "Control of Combustion-Generated Nitrogen Oxide Emissions: Technology Driven By Regulations," *Twenty-Fourth Symposium (International) on Combustion*, Combustion Institute, Pittsburgh, pp. 859-878.
2. Gupta, A. K. and Lilley, D. G., 1985, Flow field Modeling and Diagnostics, Abacus Press, Kent, UK.
3. Kamal, A., and Gollahalli, S. R., 1993, "Effects of Noncircular Fuel Nozzle on the Pollutant Emission Characteristics of Natural Gas Burner for Residential Furnaces," *Combustion, Modeling, Cofiring and NOx Control, ASME. FACT*. Vol.17, *pp*. 41-50.
4. Papanikolau, N. and Wierzba, I., 1996, "Effect of Burner Geometry on the Blowout Limits of Jet Diffusion Flames in a Co-Flowing Air Stream," *Journal of Energy Resources Technology*, Vol. 118, pp. 134-139.

5. Papanikolau, N., Wierzba, I., and Fergusson, B., 1997, ”The Structure of Jet Diffusion Flames Issuing into Co-Flowing Air Stream,” *Energy Week*, Pennwell publications, Houston, TX, Book V, pp. 222-228.

6. Turns, S. R., 2000, An Introduction to Combustion: Concepts and Applications, 2nd Edition, *McGraw-Hill Inc.*, NY.

7. Tomeczek, J., Goral, J. and Gradon, B., 1995, “Gas dynamics Abatement of NOx Emission from Industrial Natural Gas Jet Diffusion Flames,” *Combustion Science and Technology*, Vol. 105, *pp.* 55-65.

8. Cheng, T. S., Chao, Y. C., Wu, D. C., Yuan, T., Lu, C., Cheng, C., and Chang, J. M., 1998, ”Effects of Fuel-air mixing on Flame Structures and NOx Emissions in Swirling Methane Jet Flames,” *Twenty-Seventh Symposium (International) on Combustion*, University of Colorado at Boulder, Co, August 2-7.

9. Qubbaj, Ala R. and Gollahalli, S. R., 1999, ”Combustion Characteristics of Gas Jet Diffusion Flames Enveloped by a Cascade of Venturis,” *Combustion Science and Technology Journal*, Vol. 143, pp. 1-23.

10. Qubbaj, Ala R. and Gollahalli, S. R., 2000, ”Numerical Modeling of the Flow Field of a Burning Gas Jet in a Venturi-Cascade Burner,” *Energy Sources Technology Conference and Exhibition*, February 14-17, 2000, New Orleans, Louisiana, USA.

11. Lyons, V. J., 1981,” Fuel-Air Nonuniformity Effect on Nitric Oxide Emissions,” AIAA J., *Progress in Energy and Combustion*, Vol. 20, No. 5, p. 660.

12. Tangirala, V., Chen, R. H., and Driscoll, J. F., 1987, ”Effect of Heat Release and Swirl on the Recirculation within Swirl-Stabilization Flames,” *Combustion Science and Technology*, Vol. 51, pp. 75-95.

13. Chen, R. H., and Driscoll, J. F., 1988, “The Rule of the Recirculation Vortex in Improving Fuel-Air Mixing within Swirling Flames,” *Twenty-Second Symposium (International) on Combustion*, Combustion Institute, Pittsburgh, pp. 531-440.

14. Fric, T. F., 1993, ”Effects of Fuel-Air Unmixedness on NOx Emissions,” *Journal of Propulsion and Power*, Vol. 9, No. 5, p. 708.

15. Villermaux, E., 1998, " Mixing and Spray Formation in Coaxial Jets," *Journal of Propulsion and Power,* Vol. 14, No. 5, pp. 807-817.

16. Hillemans, R., Lenze, B. and Leuckel W., 1986, "Flame Stabilization and Turbulent Exchange in Strongly Swirling Natural Gas Flames," *Twenty-First Symposium (International) on Combustion*, Combustion Institute, Pittsburgh, p. 1445.

17. Charles, R. E., Emdee, J. L., Muzio, L. J. and Samuelsen, G. S., 1986, "The Effect of Inlet Conditions on the Performance and Flow field Structure of a Non-Premixed Swirl-Stabilized Distributed Reaction," *Twenty-First Symposium (International) on Combustion*, Combustion Institute, Pittsburgh, pp. 1455-1461.

18. Starner, S. H. and Bilger R. W., 1989, "Further Velocity Measurements in a Turbulent Diffusion Flame with Moderate Swirl," *Combustion Science and Technology*, Vol. 63, *pp.* 257-274.

19. Shen, D., Most, J. M., Joulain, P. and Bachman, J. S., 1994, "The Effect of Initial Condotonsfor Swirl Turbulent Diffusion Flame with a Straight-exit Burner. *Combustion Science and Technology*, Vol. 100, *pp.* 203-224.

20. Van doormaal, J. P. and Dryer, F. L., 1984, "Enhancements of the SIMPLE Methods for Predicting Incompressible Fluid Flows," *Numerical Heat Transfer,* Vol. 7, pp. 147-163.

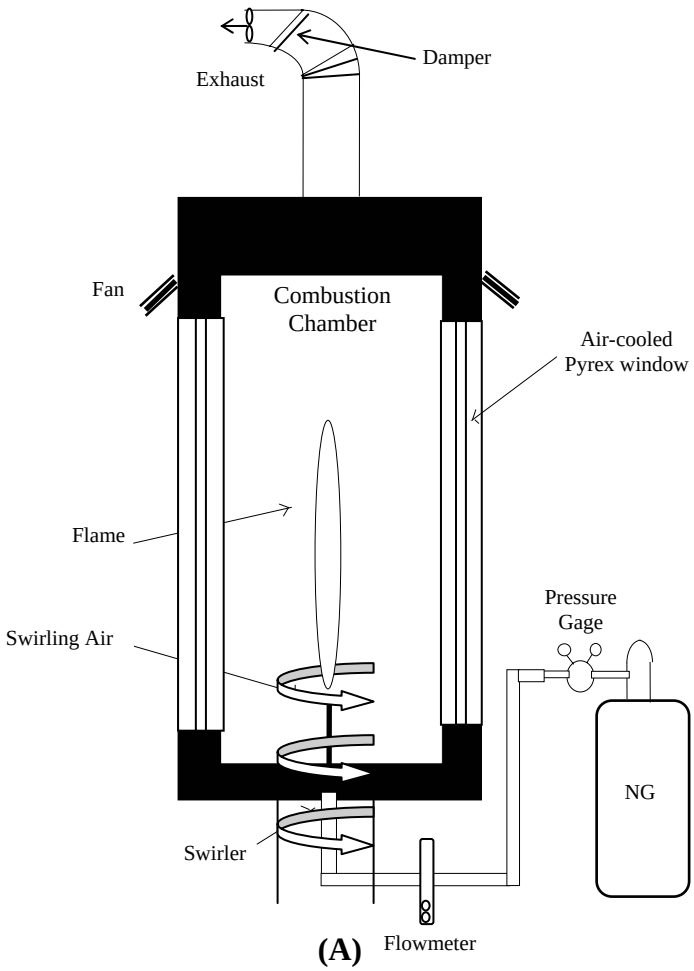

(A)

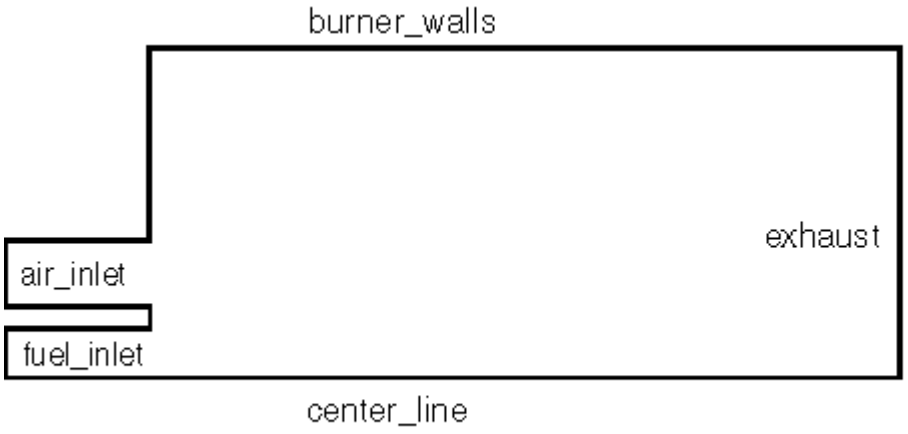

(B)

Figure1: (a) Actual physical model (b) Simplified Problem geometry

y

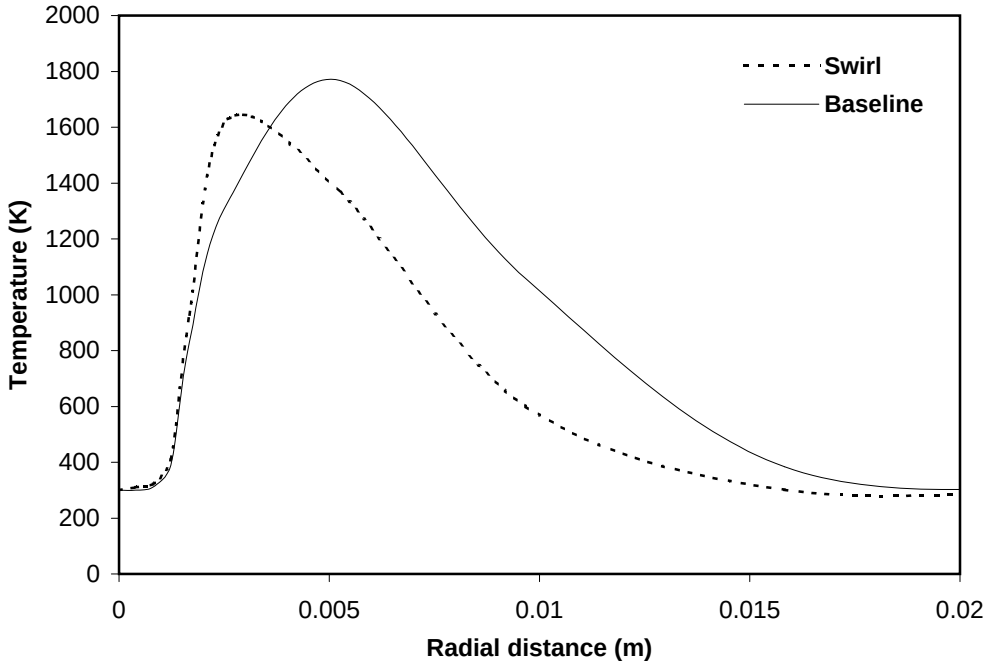

Fig. 2: Temperature Radial Profiles

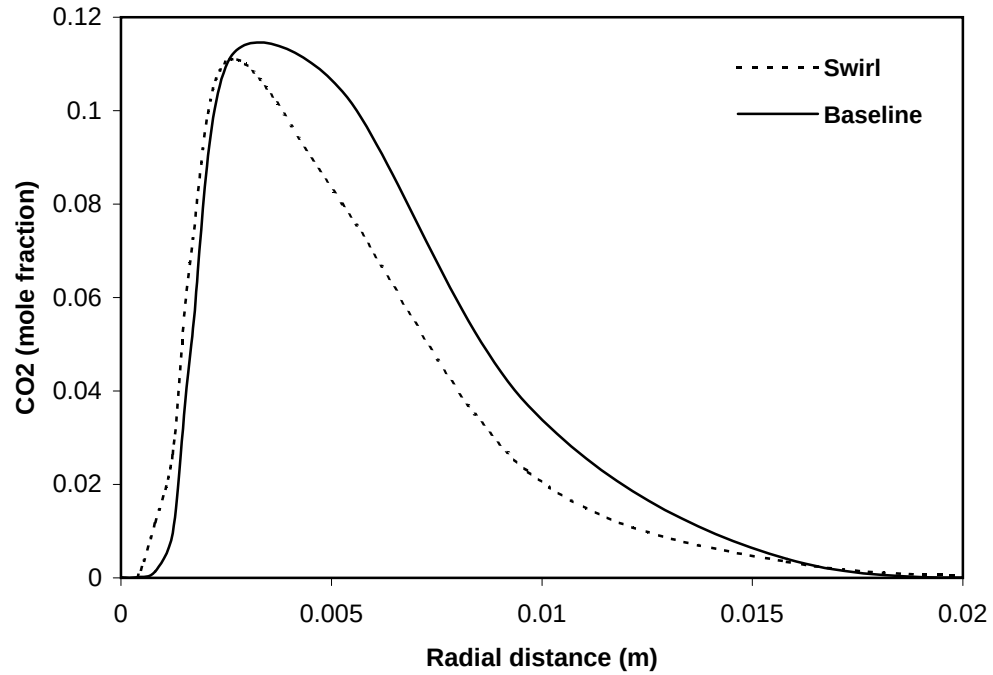

Fig. 3: Carbon Dioxide Radial Profiles

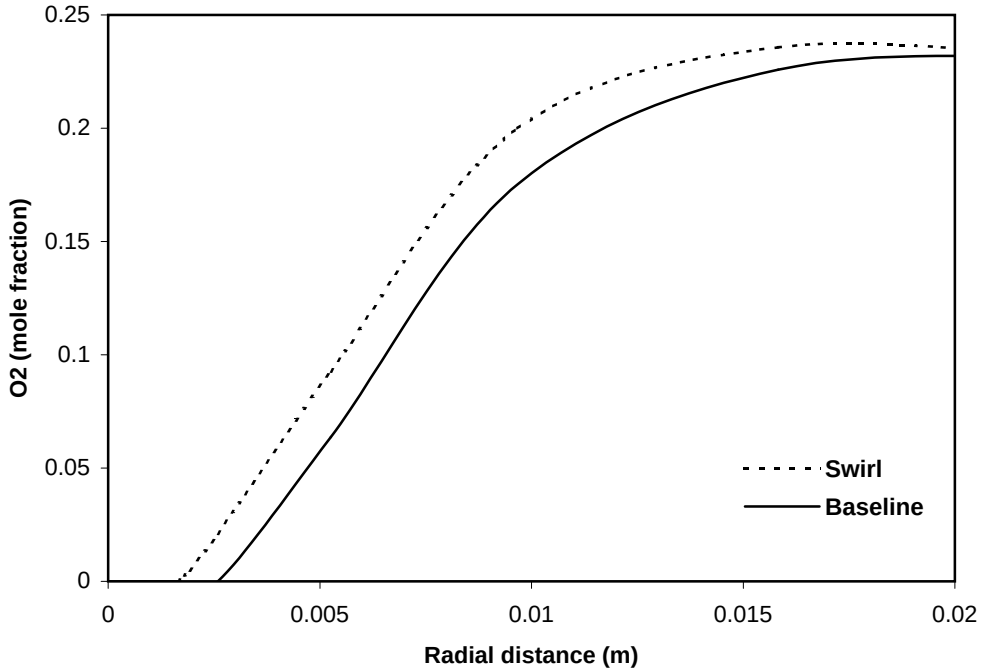

Fig. 4: Radial Oxygen Profiles

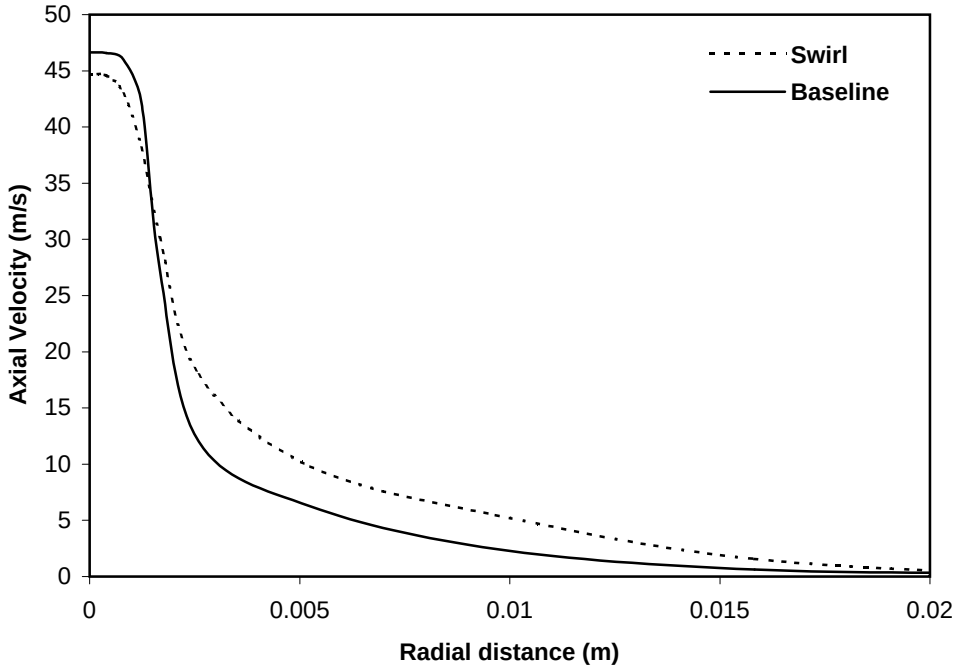

Fig. 5: Radial Profiles of Axial Velocity Component (U)

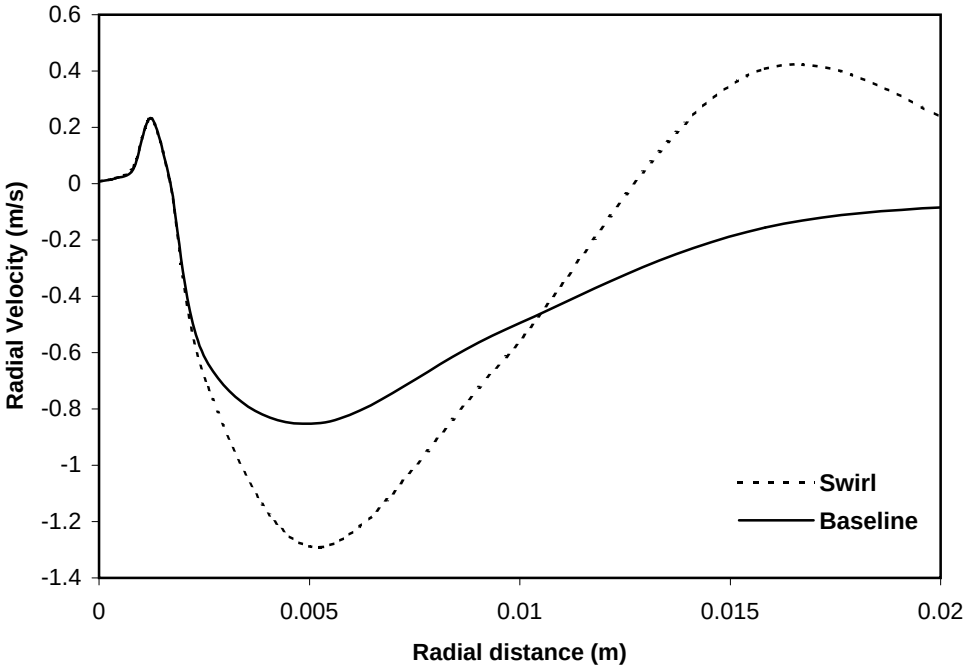

Fig. 6: Radial Profiles of Radial Velocity Component (V)

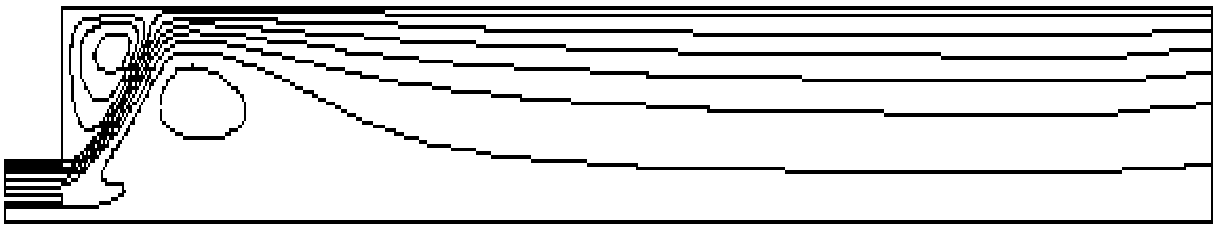

Fig. 7: Stream Function Contours